

# Identification of $\beta$ -turn and random coil amide III infrared bands for secondary structure estimation of proteins

Shuowei Cai, Bal Ram Singh<sup>1,\*</sup>

*Department of Chemistry and Biochemistry, University of Massachusetts Dartmouth, 285 Old Westport Road, Dartmouth, MA 02747, USA*

Received 23 December 1998; accepted 2 April 1999

## Abstract

Fourier transform infrared spectroscopy is increasingly becoming an important method to determine secondary structure of peptides and proteins. Among the spectral regions arising out of coupled and uncoupled stretching and bending modes of amide bonds, amide I and amide III spectral bands have been found to be the most sensitive to the variations in secondary structure folding. Amide I spectral region ( $1700\text{--}1600\text{ cm}^{-1}$ ), although most commonly used primarily because of its strong signal, suffers from several limitations, including a strong interference from water vibrational band, relatively unstructured spectral contour, and overlap of revolved bands correspondingly to various secondary structures. In contrast, amide III spectral region ( $1350\text{--}1200\text{ cm}^{-1}$ ), albeit relatively weak in signals, does not have the above limitations. Easily resolved and better defined amide III bands are quite suitable for quantitative analysis of protein secondary structure. While amide III region has been successfully used for determination of  $\alpha$ -helix and  $\beta$ -sheets (Fu, F.-N., et al. (1994) *Appl. Spectrosc.* 48, 1432–1441), bands corresponding to  $\beta$ -turns and random coils have not been identified, so far. In this paper, we describe, for the first time, identification of amide III bands corresponding to  $\beta$ -turns and random coils by selectively enhancing random coils by treatment with a denaturing reagent, and secondary structure estimation of several proteins by using the band assignments. The assignments of spectral bands were as follows:  $1330\text{--}1295\text{ cm}^{-1}$ ,  $\alpha$ -helix;  $1295\text{--}1270\text{ cm}^{-1}$ ,  $\beta$ -turns;  $1270\text{--}1250\text{ cm}^{-1}$ , random coils; and  $1250\text{--}1220\text{ cm}^{-1}$ ,  $\beta$ -sheets. The estimations of secondary structural elements by the above assignments correlated quite well with secondary structure estimations from X-ray crystallography data. © 1999 Elsevier Science B.V. All rights reserved.

**Keywords:** Amide III; Denaturation; Infrared; Proteins; Random coil; Secondary structure;  $\beta$ -Turn

\* Corresponding author. Tel.: +1-508-999-8588; fax: +1-508-999-8451.

E-mail address: bsingh@umassd.edu (B.R. Singh)

<sup>1</sup>The Henry Dreyfus Teacher-Scholar

## 1. Introduction

Elucidation of the structure of proteins and of their structure–function relationships is one of the main targets in modern biochemistry and bio-analytical chemistry. Several methods are currently used for the analysis of protein structures. Of these methods, X-ray crystallography provides the most detailed information about protein conformation and structure if high quality single crystals of protein can be prepared. However, it is usually difficult to get high quality single crystals, especially for membrane proteins. Nuclear-magnetic resonance (NMR) spectroscopy is another important tool to analyze proteins, which can provide high resolution structural information of proteins in solution. Unfortunately, NMR is a low sensitivity technique, and therefore at present, it is only restricted to small proteins < 20 kDa [1]. The practical limitations encountered in high-resolution structural techniques for proteins (e.g. X-ray crystallography and NMR methods) have stimulated progress in the development and improvement of ‘low-resolution’ spectroscopic methods, which provide global insight into the overall secondary structure of proteins without being able to establish the precise three-dimensional location of individual structural elements. One of such techniques is Fourier-transform infrared (FT-IR) spectroscopy, which is becoming an increasingly useful tool for the structural analysis of peptides and proteins.

The most important advantage of FT-IR spectroscopy is that it can readily follow the conformational change of a protein as a function of changing its environment, say from aqueous to organic solvent [2], or from detergent to lipid bilayer [3]. This advantage renders FT-IR spectroscopy especially good for probing membrane-associated proteins which are difficult to be probed by other spectroscopic techniques.

Methods currently being used to extract information on protein secondary structure from infrared spectra are based on empirical correlations between the frequencies of certain vibrational modes and types of secondary structure of polypeptide chains such as  $\alpha$ -helix,  $\beta$ -sheet,  $\beta$ -turn, and random coil. The mode most often used and

by far best characterized in this respect is the so-called amide I mode, which represents primarily the C=O stretching vibrations of amide groups and gives rise to infrared band(s) in the region between approximately 1600 and 1700  $\text{cm}^{-1}$ . Due to the strong absorption of water between 1640–1650  $\text{cm}^{-1}$ , most structures determination by amide I mode are performed in  $\text{D}_2\text{O}$  solutions. However, uncertainty in the NH/ND exchange process may cause a certain degree of ambiguity [4]. Also the serious overlapping of the random coil and the  $\alpha$ -helix band in amide I region makes it difficult to accurately predict the  $\alpha$ -helix contents in the proteins. Attempts were also made to exploit other vibrational modes, particular amide II and amide III bands. Unfortunately, even though the intensity of amide II region is relatively strong, it is not very sensitive to secondary structure changes of proteins. Furthermore, the amide II bands are strongly overlapped by bands originating from amino acid side chain vibrations [5]. On the other hand, amide III bands, which are predominantly due to the in-phase combination of N–H in-plane-bending and C–N stretching vibrations, are highly sensitive to the secondary structure [6,7]. In addition, there is no  $\text{H}_2\text{O}$  interference in this region. Therefore, even though the signal of amide III bands are  $\sim 5$ –10-fold weaker than that of amide I bands, amide III region is still very promising to estimate protein secondary structure.

In recent years, several researchers have used amide III region to determine protein structures [8–13]. Since both amide I and amide III regions are broad band, it is not possible to resolve individual bands corresponding to different secondary structure elements from the original spectra. Therefore, resolution enhancement or band narrowing methods are employed to resolve the broad overlapped band into individual bands [14]. By analyzing the spectra of proteins whose structures are already known by other methods, or by analyzing model peptides, the bands corresponding to different secondary structures can be assigned. So far, the assignment of bands in amide III region only has resolved the  $\alpha$ -helix and  $\beta$ -sheet structures [15]. The assignment of the other two major elements of protein secondary structures,  $\beta$ -turn

and random coil, is still unsolved. In this paper, we describe an approach to resolve amide III IR bands corresponding to  $\beta$ -turns and random coils. The results from our approach correlate well with the data from X-ray crystallography for  $\alpha$ -helix,  $\beta$ -sheet and  $\beta$ -turns, although the correlation for random coil structures needs further improvement.

## 2. Experimental section

### 2.1. Protein samples

The following proteins were purchased from Sigma Chemical Co. (St. Louis, MO), and used without further purification: bovine serum albumin (BSA),  $\alpha$ -chymotrypsin, concanavalin A, cytochrome *c*, hemoglobin, immunoglobulin G, lysozyme, myoglobin, ribonuclease A, and trypsin. We chose BSA,  $\alpha$ -chymotrypsin and lysozyme to study the assignment of different secondary structures because bovine serum albumin (BSA) and lysozyme are high-helix-content proteins, and  $\alpha$ -chymotrypsin which is high-sheet-content protein. Other proteins were chosen because their three-dimensional structures are known from X-ray crystallography [16].

### 2.2. Preparation of protein solutions

All protein solutions are prepared in 20-mM sodium phosphate buffer, pH 7.2. The concentration of BSA,  $\alpha$ -chymotrypsin and lysozyme used in our experiments was 5 mg ml<sup>-1</sup> for denaturation studies, and the concentration of all the proteins used in our experiments for confirming the IR spectral assignments was 1 mg ml<sup>-1</sup>.

### 2.3. Infrared measurement and data manipulation

A Nicolet Model 8210 FT-IR spectrometer, equipped with a zinc selenide attenuated total reflectance (ATR) accessory and DTGS detector, was used for spectral recordings at room temperature. The spectrometer was purged with CO<sub>2</sub>-free dry air for at least 24 h before recording spectra. For each spectrum, a 256-scan interfero-

gram was collected at a resolution of 4 cm<sup>-1</sup>. In every case, the single beam spectra of the buffer and the protein solutions were divided by the background single beam spectrum and then converted to the absorbance spectra. To obtain the protein spectra, the buffer spectra were subtracted. The following criteria were used to judge the water subtraction: a flat baseline between 2000 and 1700 cm<sup>-1</sup> and no negative lobe between this range [17,18]. The spectra then were multiplied by 100. All spectra were smoothed with a nine-point Savitsky–Golay function to remove the possible noise before further data analysis. The data were manipulated using the LabCalc 2.0 software package created by Galactic Industries (Salem, NH).

In order to examine spectral characteristics of denatured proteins, separate samples of each protein were treated with different concentrations of guanidine hydrochloride (2, 4 and 6 M). After incubation for 15 m, the protein sample was layered on the ATR crystal for spectral recording. Reference spectrum of guanidine hydrochloride corresponding to each denaturing concentration was subtracted from its respective denatured protein spectrum.

Identification of band positions was carried out by Fourier self-deconvolution. A half-bandwidth of 20 cm<sup>-1</sup> and a K-value of 2.0 were used to obtain the spectral deconvolution. Second-derivative spectra were obtained using a five-data-point window, to support the initial identification of band positions by deconvolution. The band positions obtained from the above steps were then used as the initial guess for curve-fitting of the original spectra. Best curve-fitting were obtained at the lowest possible  $\chi^2$  values.

## 3. Results and discussion

### 3.1. Denaturation studies

The chemical denaturation of each protein produces substantial alternations in the amide III bands. Specific spectral changes and structural assignments of individual proteins are described below.

### 3.1.1. Bovine serum albumin

BSA is a high- $\alpha$ -helix-content protein. Amide III spectral analysis, as shown in Fig. 1a, revealed 51%  $\alpha$ -helix (1327, 1314, 1304 and  $1298\text{ cm}^{-1}$ ), 18%  $\beta$ -sheet (1246, 1238 and  $1233\text{ cm}^{-1}$ ), and 31% other structures (1282, 1272 and  $1263\text{ cm}^{-1}$ ) for native BSA, as the method described previously [15]. This analysis is similar to the estimations from CD spectroscopy [19] and from FT-IR amide I spectral analysis [15]. After being treated with guanidine hydrochloride, the areas under bands (band strength) above  $1300\text{ cm}^{-1}$  decreased sharply and moved to the lower wave number (see Fig. 1 and Table 1). Strength of bands near  $1268$ ,  $1260$  and  $1248\text{ cm}^{-1}$  increased dramatically (see Fig. 1 and Fig. 2a). Results from NMR and CD spectroscopy have shown that during denaturation of proteins by treatment with heat or chemical denaturants, such acid, urea, and guanidine hydrochloride, the random coil structures increase [20–25]. Therefore, we can assume the bands between  $1270$  and  $1245\text{ cm}^{-1}$  arise from random coil structures. The bands below  $1245\text{ cm}^{-1}$  ( $1245$ ,  $1238$ ,  $1230$  and  $1222\text{ cm}^{-1}$ ) gradually increased from 18% to 27% after treatment with increasing concentration of guanidine hydrochloride. The strength of bands between  $1289$  and  $1270$  ( $1289$ ,  $1282$  and  $1276\text{ cm}^{-1}$ ) decreased from 21% to 15%, but the decrease was much less dramatic than the decrease in band strength above  $1300\text{ cm}^{-1}$  (see Fig. 1 and Fig. 2a). These results suggest that the  $\alpha$ -helix is very sensitive to denaturing reagent, whereas the  $\beta$ -sheet is not as sensitive to denaturing reagent. Several studies [26–28] have revealed that protein unfolding occurs via an intermediate, which maintains an unnative-like structures. Interestingly, many proteins maintain  $\beta$ -subdomain structures, in either native-like or unnative-like  $\beta$ -structures [28]. The random coil structure may also contribute to the border line spectral bands such as  $1245\text{ cm}^{-1}$  band. The other bands of amide III spectra,  $1295$ – $1270\text{ cm}^{-1}$ , could be due to  $\beta$ -turn, because the bands in this range did not increase with treatment with guanidine hydrochloride. In fact, they decreased slowly from 21% of native protein to 15% after treatment with 6 M guanidine hydrochloride. This also indicated that  $\beta$ -turn

is not very sensitive to the denaturing reagent, or may be in the intermediate state.

### 3.1.2. Lysozyme

Lysozyme is another high  $\alpha$ -helical protein. Curve-fitting analysis of amide III spectra revealed about 42%  $\alpha$ -helix ( $1316$  and  $1297\text{ cm}^{-1}$ ), 14%  $\beta$ -sheet ( $1233\text{ cm}^{-1}$ ) and 45% other structures ( $1285$ ,  $1273$ ,  $1265$  and  $1252\text{ cm}^{-1}$ ) (see Fig. 3 and Table 1). By treating with 4 M guanidine hydrochloride, the band at  $1298\text{ cm}^{-1}$  shifted down to  $1292\text{ cm}^{-1}$ , and the intensity dramatically decreased. The band at  $1235\text{ cm}^{-1}$  remained virtually unchanged. Band strength at  $1265\text{ cm}^{-1}$  increased from 1% to about 16%, the band at  $1252\text{ cm}^{-1}$  split into two bands at  $1255$  and  $1248\text{ cm}^{-1}$ . The band at  $1285\text{ cm}^{-1}$  shifted down to about  $1280\text{ cm}^{-1}$ , and the intensity increased from 3% to 14%. This increase could partly be from the disappearance of a band at  $1273\text{ cm}^{-1}$  after treatment with guanidine hydrochloride. Since the band intensity at  $1265$ ,  $1255$  and  $1248\text{ cm}^{-1}$  increased from 23% (at  $1265$  and  $1252\text{ cm}^{-1}$ ) to 42% after treatment with 4 M guanidine hydrochloride (see Fig. 2b), we tentatively assigned these bands to random coil.

### 3.1.3. $\alpha$ -Chymotrypsin

$\alpha$ -Chymotrypsin is a primarily  $\beta$ -sheet protein. The amide III spectral analysis (Fig. 4) revealed that 15%  $\alpha$ -helix ( $1323$ ,  $1311$ , and  $1304\text{ cm}^{-1}$ ); 47%  $\beta$ -sheet ( $1248$ ,  $1234$ , and  $1222\text{ cm}^{-1}$ ), and 38% other structures ( $1290$ ,  $1279$  and  $1260\text{ cm}^{-1}$ ) for native  $\alpha$ -chymotrypsin. These results are consistent with X-ray crystallography data [16]. When treated with guanidine hydrochloride, the bands above  $1300\text{ cm}^{-1}$  moved to the lower wave number and their intensities decreased. The band at  $1260\text{ cm}^{-1}$  in the native protein split into bands between  $1266$  and  $1250\text{ cm}^{-1}$ . The band at  $1248$ – $1249\text{ cm}^{-1}$  dramatically increased in strength from 20% to 38%. This indicated that band at  $1249\text{ cm}^{-1}$  represented a borderline assignment between random coil and  $\beta$ -sheet. The intensity of bands at  $1290$  and  $1282\text{ cm}^{-1}$  also decreased from 20% to 11% after treatment with 6 M guanidine hydrochloride (see Fig. 2c and Table 1). The effect of guanidine hydrochloride

Table 1

Infrared band positions in the amide III spectral region of various proteins in their native state and in the denatured state created by different concentrations of guanidine hydrochloride<sup>a</sup>

Proteins and conditions		Band position <sup>b</sup>	Area <sup>b</sup> (%)	Assignment
BSA	Native solution	1327 ± 1	13 ± 3	α-Helix
		1314 ± 0	19 ± 3	α-Helix
		1308 ± 0	0 ± 0	α-Helix
		1304 ± 2	3 ± 1	α-Helix
		1298 ± 2	16 ± 2	α-Helix
		1282 ± 2	16 ± 5	Turn
		1272 ± 0	5 ± 1	Turn
		1263 ± 1	10 ± 1	Random Coil
		1246 ± 1	15 ± 2	β-Sheet
		1238 ± 0	2 ± 1	β-Sheet
		1233 ± 2	1 ± 1	β-Sheet
	2 M GuHCl solution	1323 ± 2	8 ± 1	α-Helix
		1314 ± 1	14 ± 3	α-Helix
		1301 ± 2	13 ± 4	α-Helix
		1285 ± 1	15 ± 1	Turn
		1263 ± 1	19 ± 4	Random Coil
		1246 ± 1	15 ± 2	β-Sheet
		1238 ± 0	2 ± 1	β-Sheet
		1233 ± 2	1 ± 1	β-Sheet
	4 M GuHCl solution	1333 ± 0	1 ± 1	α-Helix
		1318 ± 1	12 ± 2	α-Helix
		1306 ± 1	11 ± 2	α-Helix
		1296 ± 0	6 ± 1	α-Helix/Turn
		1282 ± 1	14 ± 2	Turn
		1270 ± 2	6 ± 1	Random Coil
		1260 ± 2	12 ± 1	Random Coil
		1247 ± 1	14 ± 2	Random Coil
		1236 ± 0	19 ± 3	β-Sheet
		1222 ± 2	6 ± 2	β-Sheet
	6 M GuHCl solution	1325 ± 0	3 ± 1	α-Helix
		1314 ± 0	10 ± 0	α-Helix
		1302 ± 2	6 ± 1	α-Helix
		1289 ± 1	9 ± 1	Turn
		1276 ± 1	6 ± 0	Turn
		1268 ± 0	6 ± 2	Random Coil
		1259 ± 0	14 ± 1	Random Coil
		1248 ± 2	20 ± 2	Random Coil
		1235 ± 1	19 ± 2	β-Sheet
		1222 ± 2	8 ± 2	β-Sheet
Lysozyme <sup>c</sup>	Native solution	1316 ± 2	19 ± 3	α-Helix
		1298 ± 2	24 ± 4	α-Helix
		1285 ± 2	3 ± 2	Turn
		1273 ± 1	15 ± 2	Turn
		1265 ± 2	1 ± 3	Random Coil
		1252 ± 1	22 ± 2	Random Coil/β-Sheet
		1233 ± 2	16 ± 5	β-Sheet

Table 1 (Continued)

Lysozyme <sup>c</sup>	2 M GuHCl solution	1319 ± 1	11 ± 2	α-Helix
		1306 ± 1	8 ± 2	α-Helix
		1297 ± 2	10 ± 2	α-Helix
		1285 ± 0	10 ± 2	Turn
		1271 ± 2	16 ± 1	Random Coil/Turn
		1257 ± 0	18 ± 1	Random Coil
		1248 ± 1	9 ± 1	Random Coil/β-Sheet
		1235 ± 0	18 ± 2	β-Sheet
	4 M GuHCl solution	1316 ± 1	4 ± 1	α-Helix
		1310 ± 1	12 ± 2	α-Helix
		1292 ± 1	10 ± 2	Turn
		1280 ± 1	14 ± 3	Turn
		1265 ± 1	17 ± 4	Random Coil
		1255 ± 2	11 ± 5	Random Coil
		1247 ± 1	14 ± 5	Random Coil/β-Sheet
		1235 ± 0	17 ± 3	β-Sheet
	Native solution	1316 ± 2	19 ± 3	α-Helix
		1298 ± 2	24 ± 4	α-Helix
		1285 ± 2	3 ± 2	Turn
		1273 ± 1	15 ± 2	Turn
		1265 ± 2	1 ± 3	Random Coil
		1252 ± 1	22 ± 2	Random Coil/β-Sheet
		1233 ± 2	16 ± 5	β-Sheet
	2 M GuHCl solution	1319 ± 1	11 ± 2	α-Helix
		1306 ± 1	8 ± 2	α-Helix
		1297 ± 2	10 ± 2	α-Helix
		1285 ± 0	10 ± 2	Turn
		1271 ± 2	16 ± 1	Random Coil/Turn
		1257 ± 0	18 ± 1	Random Coil
		1248 ± 1	9 ± 1	Random Coil/β-Sheet
		1235 ± 0	18 ± 2	β-Sheet
	4 M GuHCl solution	1316 ± 1	4 ± 1	α-Helix
		1310 ± 1	12 ± 2	α-Helix
		1292 ± 1	10 ± 2	Turn
		1280 ± 1	14 ± 3	Turn
		1265 ± 1	17 ± 4	Random Coil
		1255 ± 2	11 ± 5	Random Coil
		1247 ± 1	14 ± 5	Random Coil/β-Sheet
		1235 ± 0	17 ± 3	β-Sheet
α-Chymotrypsin	Native solution	1323 ± 1	4 ± 1	α-Helix
		1311 ± 0	9 ± 3	α-Helix
		1304 ± 1	2 ± 1	α-Helix
		1290 ± 2	7 ± 2	Turn
		1279 ± 1	13 ± 2	Turn
		1260 ± 2	18 ± 5	Random Coil
		1248 ± 0	20 ± 4	Random Coil/β-Sheet
		1234 ± 1	22 ± 5	β-Sheet
		1222 ± 1	5 ± 2	β-Sheet

Table 1 (Continued)

Proteins and conditions	Band position <sup>b</sup>	Area <sup>b</sup> (%)	Assignment
2 M GuHCl solution	1329 ± 1	6 ± 2	α-Helix
	1316 ± 1	7 ± 2	α-Helix
	1300 ± 2	2 ± 1	α-Helix
	1288 ± 1	8 ± 4	Turn
	1277 ± 1	7 ± 2	Turn
	1263 ± 2	14 ± 3	Random coil
	1251 ± 0	21 ± 3	Random coil/β-Sheet
	1236 ± 1	27 ± 4	β-Sheet
4 M GuHCl solution	1221 ± 0	8 ± 4	β-Sheet
	1318 ± 0	6 ± 1	α-Helix
	1304 ± 1	3 ± 1	α-Helix
	1286 ± 1	10 ± 1	Turn
	1274 ± 1	8 ± 2	Turn
	1261 ± 2	17 ± 3	Random coil
	1249 ± 0	23 ± 3	Random coil/β-Sheet
	1235 ± 1	28 ± 1	β-Sheet
6 M GuHCl solution	1218 ± 1	5 ± 2	β-Sheet
	1309 ± 1	12 ± 2	α-Helix
	1290 ± 1	1 ± 0	Turn
	1282 ± 2	10 ± 2	Turn
	1266 ± 2	2 ± 0	Random coil
	1260 ± 1	2 ± 1	Random coil
	1257 ± 2	10 ± 2	Random coil
	1249 ± 1	38 ± 1	Random coil
	1236 ± 0	20 ± 3	β-Sheet
	1219 ± 0	5 ± 1	β-Sheet

<sup>a</sup>Band areas were determined by curve-fitting.

<sup>b</sup>The ± values are the standard deviations calculated by three individual spectra in each case.

<sup>c</sup>The 6 M guanidine hydrochloride solution leads the lysozyme to precipitation.

on bands at 1234 and 1222 cm<sup>-1</sup> was not significant. Therefore, it supported our earlier assertion that α-helix was more sensitive to denaturing reagent than β-sheet. The bands between 1295 and 1271 cm<sup>-1</sup> (1290, 1279 for native protein, and shifted bands at 1290 and 1282 cm<sup>-1</sup> after treatment with 6 M guanidine hydrochloride) decreased from 20% to 11%. Therefore this region was tentatively assigned to β-turn.

### 3.2. Infrared band assignment and secondary structure estimation

From the amide III spectral analysis of BSA, lysozyme and α-chymotrypsin, we observed that after treatment with guanidine hydrochloride, the strengths of bands between 1248 and 1270 cm<sup>-1</sup>

dramatically increased and the intensity of bands between 1330 and 1295 cm<sup>-1</sup> decreased sharply. Intensity of bands between 1245 and 1220 cm<sup>-1</sup>, and between 1294 and 1271 cm<sup>-1</sup>, gradually decreased with increased concentration of guanidine hydrochloride. Since guanidine hydrochloride is a denaturing reagent, the random coils in a protein increases after treatment with increasing concentration of guanidine hydrochloride. Based on these results, we tentatively assigned the bands between 1270 and 1250 cm<sup>-1</sup> to random coils. Fu et al. [15] previously reported that the bands above 1300 cm<sup>-1</sup> correspond to α-helix and the bands below 1245 cm<sup>-1</sup> correspond to β-sheet. Therefore, we can derive that bands between 1294 and 1271 cm<sup>-1</sup> are due to β-turns. The intensity of this region also decreased gradually

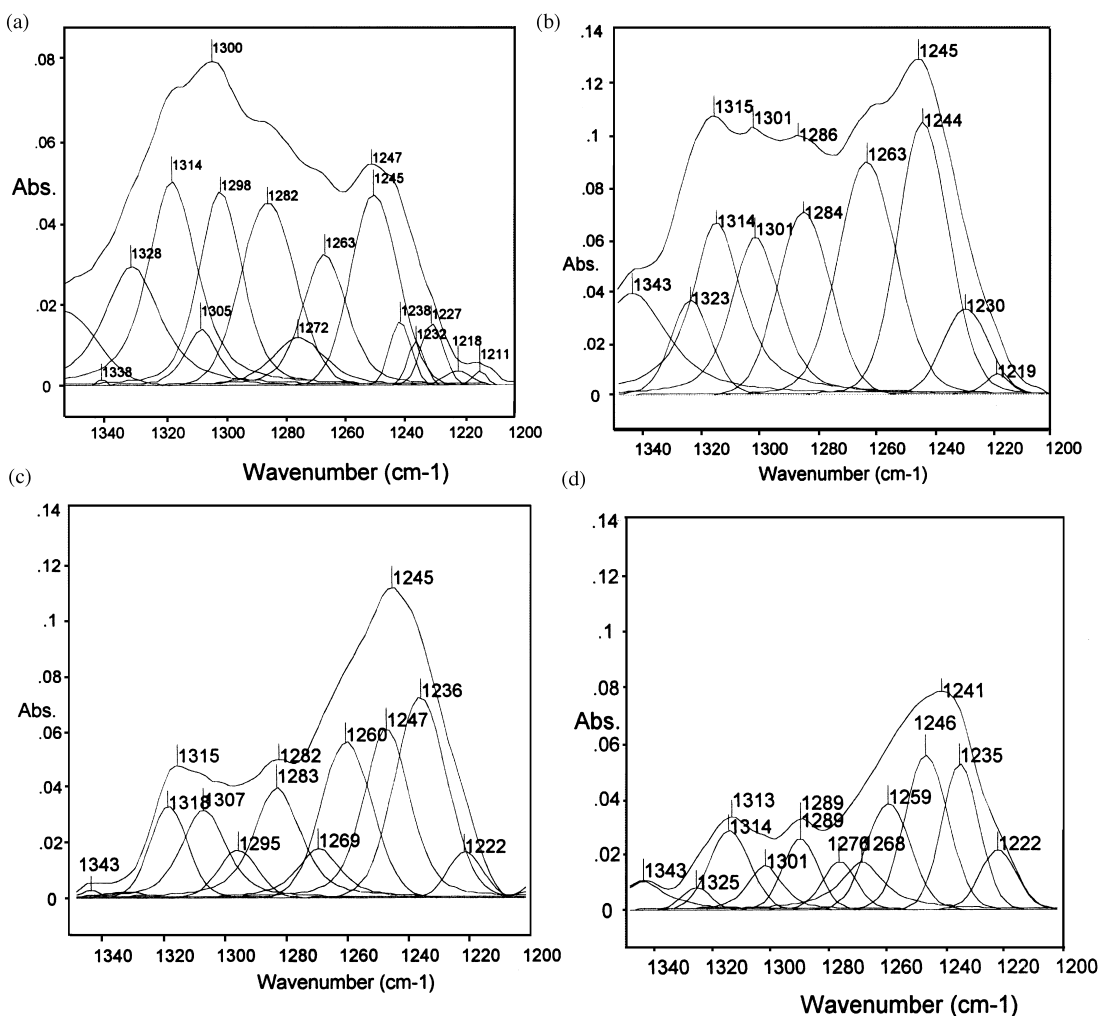


Fig. 1. Curve-fitting analysis of FT-IR spectra of BSA in amide III region. Panel a: native BSA; Panel b: BSA treated with 2 M guanidine hydrochloride; Panel c: BSA treated with 4 M guanidine hydrochloride; Panel d: BSA treated with 6 M guanidine hydrochloride.

when treated with guanidine hydrochloride (see Table 1), which would not be observed if these bands originated in random coil structures. The gradual decrease of  $\beta$ -turn after treatment with guanidine hydrochloride may indicate that the intermediate of unfolded protein may still retain  $\beta$ -turn structures as well as  $\beta$ -sheet structures [28]. The bands between 1300 and 1295  $\text{cm}^{-1}$  may be due to either  $\alpha$ -helix or  $\beta$ -turn, or a mixture of these two structures, a structure between these two structural forms. The bands in the boundary

spectral region between 1245 and 1250  $\text{cm}^{-1}$  may be due to either random coil or  $\beta$ -sheet, or a mixture of these two structures, a structure between these two forms.

Our results also indicate that the  $\alpha$ -helix is very sensitive to the denaturing reagent. However, the  $\beta$ -sheet and  $\beta$ -turn structures are not. One reason for  $\beta$ -sheet not being very sensitive to denaturing reagent is that the proteins may form some inter-molecular  $\beta$ -sheet structures in the presence of denaturing reagents or form the interme-



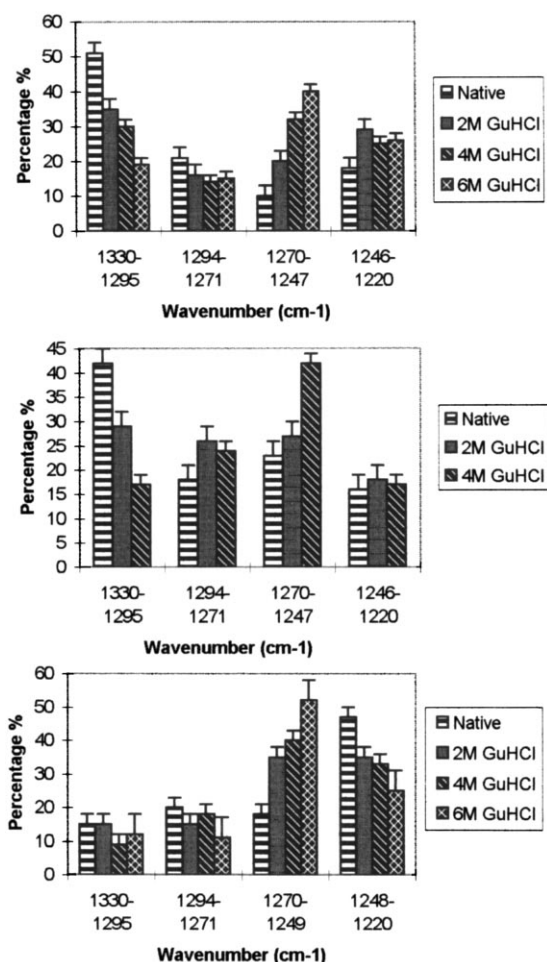


Fig. 2. Relative combined band strength (%) of different amide III spectral regions before and after treatment with guanidine hydrochloride. Panel a: BSA; Panel b: lysozyme; Panel c: α-chymotrypsin. Error bars represent the S.D. calculated for three different spectral recordings.

diate when the protein is under going the unfolding process [28]. This observation is consistent with the results from thermal denaturation of globular proteins studied by Anderle and Mendelsohn [6].

In order to confirm our spectral band assignments described above, we collected IR spectra of a total of nine different proteins, whose secondary structures have been known from X-ray crystallographic studies. The results of secondary structure estimation based on amide III spectral

analysis of all the proteins are listed in Table 2. In Table 2, we have also listed the secondary structures of these proteins from the analysis of amide I FT-IR and CD spectra of these proteins carried out by other researchers.

In order to assess the correlation between secondary structure estimation based on amide III IR spectra and secondary structure estimated from X-ray crystallography, we performed the statistical tests to derive significant correlations. The protein secondary structure from curve-fitting analysis were compared with the data from X-ray crystallography by computing the Pearson correlation coefficients (PCC) and standard deviations (S) [35].

$$\text{PCC} = \left( N \sum x_i y_i - \sum x_i \sum y_i \right) / \left\{ \left[ N \sum x_i^2 - \left( \sum x_i \right)^2 \right]^{1/2} \times \left[ N \sum y_i^2 - \left( \sum y_i \right)^2 \right]^{1/2} \right\}$$

$$S = \left[ \sum (x_i - y_i)^2 / (N - 1) \right]^{1/2}$$

where  $x_i$  is the result from curve fitting, and  $y_i$  is the result from X-ray studies. The statistical test results are listed in Table 3. For a perfect correlation, PCC of 1.0 and S of 0 is expected.

The correlation between band assignment in amide III region and X-ray data is very good for α-helix and β-sheet (see Fig. 5 and Table 3). However, for β-turn and random coil, the correlation coefficient is much lower. Even though the β-turn estimation from amide III spectral band analysis is significantly correlated with that from X-ray crystallographic study (the critical value of PCC is 0.602 with 95% confidence for nine samples), the estimation of β-turn and random coil is not correlated as well with X-ray crystallographic study as the α-helix and β-sheet estimations. This is partly due to the narrow range of β-turn and random coil contents in the standard proteins analyzed for this study. Another reason for poor estimation of random coil is the fact that the random coil structures are not defined very well in X-ray crystallographic studies [36,37], and are

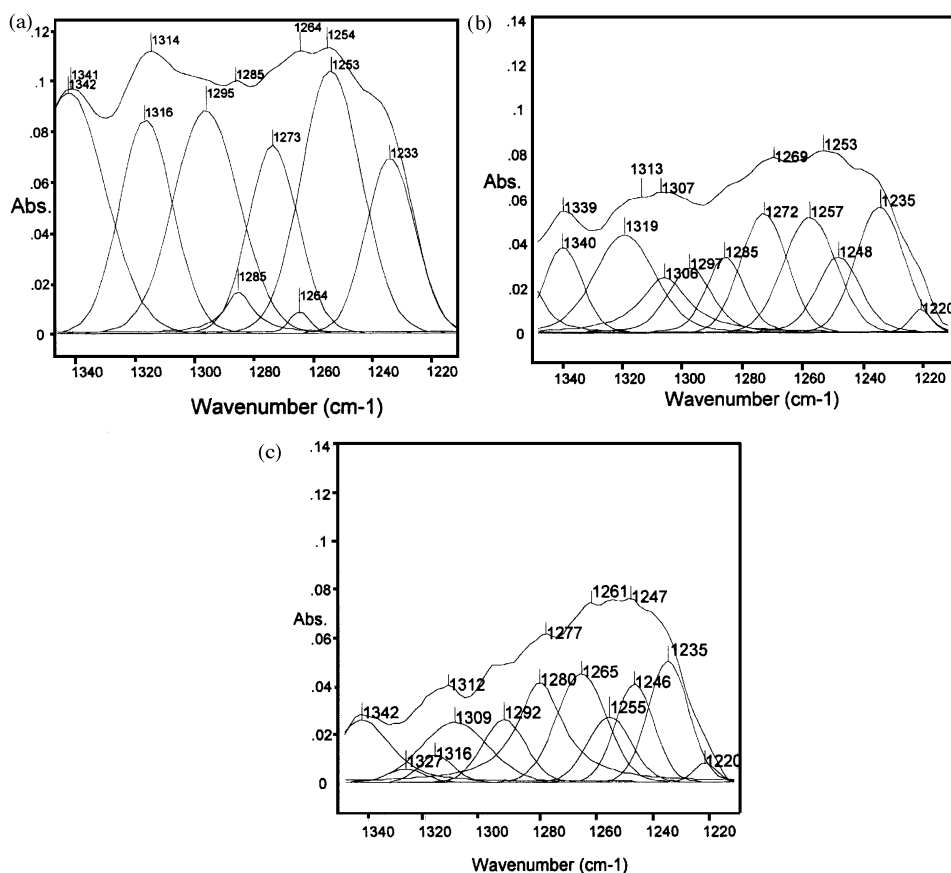


Fig. 3. Curve-fitting analysis of FT-IR spectra of lysozyme in amide III region. Panel a: native lysozyme; Panel b: lysozyme treated with 2 M guanidine hydrochloride; Panel c: lysozyme treated with 4 M guanidine hydrochloride.

usually referred to the structures difficult to describe using traditional secondary structure classification. Most algorithms for protein conformational analysis from X-ray crystallography are based on the template matching method, which consists of defining a structure template based on  $\alpha$ -carbon distances,  $\alpha$ -carbon torsion angles,  $\phi$ - $\psi$  angles, hydrogen bond, geometric features, and other parameters [16]. The random coils are usually referred to the conformations that do not match the template. Thus, different estimates of random coils result when using different templates [38]. Therefore, the estimation of random coil structures from X-ray crystallography is not very reliable.

Our data also agreed with the results obtained from amide I FT-IR spectra by Dong et al. [29],

and our results of turn and random coil contents were closer to these amide I results rather than the X-ray data. It is possible that part of the difference in secondary structure contents derived from IR spectroscopy and X-ray crystallography may originate from a differential solution and crystal structures of proteins. Such differences have been documented for several proteins in the literatures [10,39,40].

Our results showed that the curve fitting of amide III region of protein IR spectra provided a very good estimation of protein secondary structure. There are, however, a number of problems associated with the curve-fitting procedure. One of these is that the band assignment method is based on the assumption that the molar absorptivities of the bands associated with different sec-

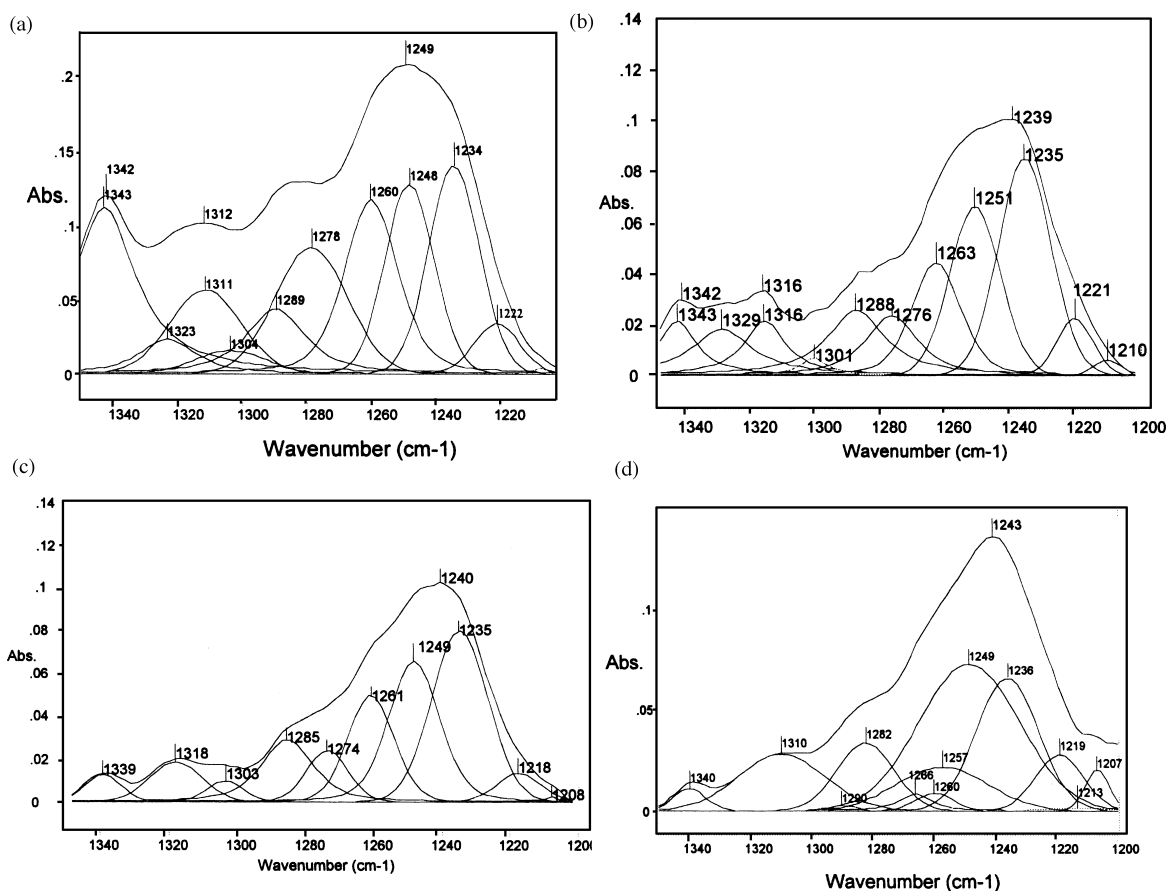


Fig. 4. Curve-fitting analysis of FT-IR spectra of  $\alpha$ -chymotrypsin in amide III region. Panel a: native  $\alpha$ -chymotrypsin; Panel b:  $\alpha$ -chymotrypsin treated with 2 M guanidine hydrochloride; Panel c:  $\alpha$ -chymotrypsin treated with 4 M guanidine hydrochloride; Panel d:  $\alpha$ -chymotrypsin treated with 6 M guanidine hydrochloride.

ondary structural elements are assumed to be identical. The correlation study done by Susi and Byler [14] suggested that this may be a reasonable assumption. Studies on poly-L-lysine have shown that the molar absorptivities of different secondary structures are, however, significantly different [41]. Another problem of this method is that there is a significant element of subjectivity associated with curve-fitting, such as initial choice of input parameters. The deconvolution also should be handled with care. Over-deconvolution produces negative side lobes on absorption and may result in artificial bands from noise. For this reason, we routinely use second-derivative to confirm our initial peak positions determined from

the deconvolution process. Our previous work [15] showed that a combination of these two techniques can be successfully used to choose initial peak positions for curve-fitting. Because amide III region generally presents a more feature spectral contour [42], the resolution of bands is easier in this region compared to the amide I region. The interference from the side chain is also a concern in the use of amide III region. However, the results from our current work and from our previous work [15] indicated that side chain effect is not a major problem for the use of amide III region, and the assignment results from amide III region are acceptable. Since amide III region avoids the interference from  $H_2O$ , it is very

Table 2

Comparison of protein secondary structures determined by curve-fitting of amide III region of protein IR spectra and X-ray crystallography

Protein	$\alpha$ -Helix	$\beta$ -Sheet	$\beta$ -Turn	Random coil	Method <sup>a</sup>
$\alpha$ -Chymotrypsin	15	47	20	18	Current method
	8	50	27	15	X-Ray [16]
	9	47	30	14	IR-amide I [29]
	8–15	10–53	2–22	38–70	CD [30–34]
Concanavalin A	18	49	25	8	Current method
	3	60	22	15	X-Ray [16]
	8	58	26	8	IR-amide I [29]
	3–25	41–49	15–27	9–36	CD [30–34]
Cytochrome <i>c</i>	43	15	26	15	Current method
	48	10	17	25	X-Ray [16]
	42	21	25	12	IR-amide I [29]
	27–46	0–9	15–28	28–41	CD [30–32]
Hemoglobin	65	4	11	20	Current method
	87	0	7	6	X-Ray [16]
	78 <sup>b</sup>	12	10		IR-amide I [29]
	68–75	1–4	15–20	9–16	CD [30,34]
IgG	10	60	17	13	Current method
	3	67	18	12	X-Ray [16]
	3	64	28	5	IR-amide I [29]
Lysozyme	43	16	18	23	Current method
	45	19	23	13	X-Ray [16]
	40	19	27	14	IR-amide I [29]
Myoglobin	61	11	7	21	Current method
	85	0	8	7	X-Ray [16]
	85 <sup>b</sup>	0	8	7	IR-amide I [29]
	67–86	0–13	0–6	11–30	CD [30–32]
Ribonulcease A	21	41	25	12	Current method
	23	46	21	10	X-Ray [16]
	15	40	36	9	IR-amide I [29]
	13–30	21–44	11–22	19–50	CD [30–32]
Trypsin	14	49	23	13	Current method
	9	56	24	11	X-Ray [16]
	9	44	38	9	IR-amide I [29]

<sup>a</sup>The numbers in parentheses are reference numbers.

<sup>b</sup>The sum of  $\alpha$ -helix and random coil.

promising to be used in determination of membrane or lipid-associated proteins, for which subtraction of the H<sub>2</sub>O band is known to be very difficult [43].

#### 4. Conclusions

Experimental observations presented in this article clearly show that amide III spectral region is

Table 3

Comparison of the statistical parameters of current method and X-ray data

	$\alpha$ -Helix	$\beta$ -Sheet	$\beta$ -Turn	Random coil
PCC	0.989	0.989	0.684	0.339
S	0.13	0.077	0.054	0.085

quite sensitive to the protein secondary structures and can be effectively used for their estimation. Unlike the amide I vibration, which occurs at about the same frequency ( $1645\text{--}1655\text{ cm}^{-1}$ ) for  $\alpha$ -helical and random coil structures, the amide III vibrations are clearly able to distinguish these two classes of secondary structure. The following frequency ranges are considered the best available at present for the correlation of amide III modes with secondary structure:  $1330\text{--}1295\text{ cm}^{-1}$ ,  $\alpha$ -helix;  $1295\text{--}1270\text{ cm}^{-1}$ ,  $\beta$ -turn;  $1270\text{--}1250\text{ cm}^{-1}$ , random coil;  $1245\text{--}1220\text{ cm}^{-1}$ ,  $\beta$ -sheet. The boundary region of  $1245\text{--}1250\text{ cm}^{-1}$  may have contributions from both random coil and

$\beta$ -sheet structures; the boundary region of  $1300\text{--}1295\text{ cm}^{-1}$  may have contributions from both  $\alpha$ -helix and  $\beta$ -turn structures. Applying data processing methods to the amide III spectral region eliminates the concerns of water interference and the ambiguity in identifying the  $\alpha$ -helix and random coil bands, in contrast to the amide I region. In addition, amide III is more sensitive to protein secondary structures. Although the amide III mode is  $\sim 5\text{--}10$ -fold weaker in IR band strength than the amide I mode, it is detectable with modern instrumentation. Thus the amide III region of protein IR spectra appears to be a valuable tool in estimating individual protein secondary structural contents. Our current work presents the amide III region to be a complementary method to amide I analysis in protein structural studies.

### Acknowledgements

This study was in part supported by a grant

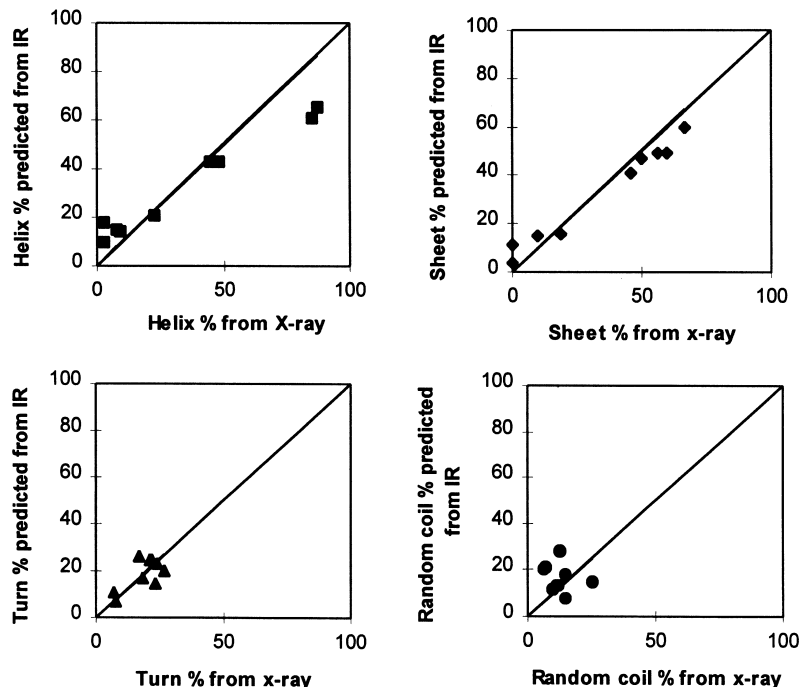


Fig. 5. Correlation of secondary structure determined by band assignment from amide III region with values from X-ray crystallography determined by Levitt and Greer [16].

(NS33740) from National Institutes of Health — National Institute of Neurological Disorders and Stroke.

## References

- [1] G. Wagner, *Nature Struct. Biol.* 4 (1997) 841.
- [2] K. Griebenow, A.M. Klibanov, *J. Am. Chem. Soc.* 118 (1996) 11695.
- [3] Y.P. Zhang, R.N.A.H. Lewis, G.D. Henry, B.D. Sykes, R.S. Hodges, R.N. McElhaney, *Biochemistry* 34 (1995) 2348.
- [4] S.W. Englander, N.W. Downer, H. Teitelbaum, *Ann. Rev. Biochem.* 41 (1972) 903.
- [5] Y.N. Chirgadze, O.V. Fedorov, N.P. Trushina, *Biopolymers* 14 (1975) 679.
- [6] G. Anderle, R. Mendelsohn, *Biophys. J.* 52 (1987) 69.
- [7] K. Kaiden, T. Matsui, S. Tanaka, *Appl. Spectrosc.* 41 (1987) 861.
- [8] B.R. Singh, M.P. Fuller, G. Schiavo, *Biochem. J.* 46 (1990) 155.
- [9] B.R. Singh, D.B. DeOliveira, F.-N. Fu, M.P. Fuller, *Proc. Biomol. Spectr.* III 1890 (1993) 47.
- [10] B.R. Singh, F.-N. Fu, D.N. Ledoux, *Nature Struct. Biol.* 1 (1994) 358.
- [11] K. Griebenow, A.M. Klibanov, *Proc. Natl. Acad. Sci. USA* 92 (1995) 10966.
- [12] H.R. Costantino, K. Griebenow, P. Mishra, R. Langer, A.M. Klibanov, *Biochim. Biophys. Acta* 1253 (1995) 69.
- [13] E. Bramanti, E. Benedetti, A. Sagripanti, F. Papineschi, E. Benedetti, *Biopolymers* 41 (1997) 545.
- [14] H. Susi, D.M. Byler, *Meth. Enzymol.* 130 (1986) 290.
- [15] F.-N. Fu, D.B. DeOliveira, W. Trumble, H.K. Sarkar, B.R. Singh, *Appl. Spectrosc.* 48 (1994) 1432.
- [16] M. Levitt, J. Greer, *J. Mol. Biol.* 114 (1977) 181.
- [17] P.I. Haris, D.C. Lee, D. Chapman, *Biochim. Biophys. Acta* 874 (1986) 255.
- [18] R.C. Mitchell, P.I. Haris, C. Fallowfield, D.J. Keeling, D. Chapman, *Biochim. Biophys. Acta* 941 (1988) 31.
- [19] E. Schechter, E.R. Blout, *Proc. Natl. Acad. Sci. USA* 51 (1964) 695.
- [20] F. Ahmad, P. McPhie, *Int. J. Pept. Protein Res.* 12 (1978) 155.
- [21] B.B. Kitchell, R.W. Henkens, *Int. J. Pept. Protein Res.* 14 (1979) 21.
- [22] J.J. Osterhout Jr., K. Muthukrishnan, B.T. Nall, *Biochemistry* 24 (1985) 6680.
- [23] P.P. Batra, K. Sasa, T. Ueki, K. Takeda, *J. Protein Chem.* 8 (1989) 221.
- [24] H. Fabian, C. Schultz, D. Naumann, O. Landt, U. Hahn, W. Saenger, *J. Mol. Biol.* 232 (1993) 967.
- [25] A.W. Vermeer, M.G. Bremer, W. Norde, *Biochim. Biophys. Acta* 1425 (1998) 1.
- [26] K. Oberg, B.A. Chrnyk, R. Wetzel, A.L. Fink, *Biochemistry* 33 (1994) 2628.
- [27] A.L. Fink, *Annu. Rev. Biophys. Biomol. Struct.* 24 (1995) 495.
- [28] A.L. Fink, *Fold Des.* 3 (1998) 9.
- [29] A. Dong, P. Huang, W.S. Caughey, *Biochemistry* 29 (1990) 3303.
- [30] J.P. Hennessey Jr., C. Johnson Jr, *Biochemistry* 20 (1981) 1085.
- [31] S. Provencher, J. Glockner, *Biochemistry* 20 (1981) 33.
- [32] C.-T. Chang, C.-S. Wu, T.-J. Tang, *Anal. Biochem.* 91 (1978) 13.
- [33] S. Brahms, J. Brahms, *J. Mol. Biol.* 138 (1980) 149.
- [34] P. Manavalan, W.C. Johnson, Jr., *Anal. Biochem.* 167 (1987) 76.
- [35] N.N. Kalnin, I.A. Baikalov, S.Y.U. Venyaminov, *Biopolymers* 30 (1990) 1273.
- [36] J.S. Fetrow, M.H. Zehfus, G.D. Rose, *Biotechnology* 6 (1988) 167.
- [37] J.F. Lesczynski, R.D. Rose, *Science* 234 (1986) 849.
- [38] W. Kabsch, C. Sander, *Biopolymers* 22 (1983) 2577.
- [39] B.R. Singh, M.L. Evenson, M.S. Bergdoll, *Biochemistry* 27 (1988) 8735.
- [40] B.R. Singh, M.J. Betley, *J. Biol. Chem.* 264 (1989) 4404.
- [41] M. Jackson, P.I. Haris, D. Chapman, *J. Mol. Struct.* 224 (1989) 329.
- [42] R.J. Jakobsen, F.M. Wasacz, *Appl. Spectrosc.* 44 (1990) 1478.
- [43] Y. Hu, B.R. Singh, *Appl. Spectrosc.* 45 (1995) 1356.